Structural Features of Random Polyester−Amide Copolymers As Revealed by X-ray Scattering and Microindentation Hardness

A. Flores,[†] D. Pietkiewicz,[‡] N. Stribeck,[§] Z. Roslaniec,[‡] and F. J. Baltá Calleja*,[†]

Instituto de Estructura de la Materia (CSIC), Serrano 119, 28006 Madrid, Spain; Institute of Materials Engineering, Technical University of Szczecin, Av. Piastow 17, 70-130 Szczecin, Poland; and Institut für Technische und Makromolekulare Chemie der Universität Hamburg, Hamburg, Germany

Received February 5, 2001

ABSTRACT: The correlation between nanostructure, as derived by X-ray scattering, and the micromechanical properties, as revealed by microindentation hardness, of a series of novel random ester−amide copolymers, based on butyl terephthalate and an etherdiamide, has been investigated. The interface distribution function has been used for the analysis of the small-angle X-ray data. The influence of the etherdiamide content and the number of the flexible groups in the etherdiamide unit on the nanostructure of the copolyester−amides is discussed. Hardness is shown to be a property critically dependent on the number of etherdiamide sequences within the copolymer chains. The hardness values of the copolyesters appear to deviate from the linear additivity law. This deviation seems to be mainly due to a contribution of several factors: (i) the lower hardness value of the poly(butyl terephthalate) (PBT) amorphous segments within the copolymer with respect to that of the PBT homopolymer; (ii) an increase in the surface free energy of the PBT crystals with increasing etherdiamide content; (iii) a decrease in the energy required for the mechanical deformation of the PBT crystals with increasing etherdiamide content and increasing number of flexible groups within the etherdiamide unit.

Introduction

Flexible copolyester−amides have been the subject of extensive research in the past years, especially those containing aromatic−aliphatic spacers.[1−7] Depending on the synthesis method, alternating copolymers, segmented block copolymers, or random copolymers are obtained. The behavior of regularly alternating copolyester−amides usually resembles that of a homopolymer, exhibiting glass transition, T_g, and melting temperature, T_m, values lying in between those of the constituent polyesters and polyamides. Some of these materials have been found to develop thermotropic mesomorphicity, despite their aromatic rings being well separated by strictly alternating aliphatic groups.[1] Furthermore, the length of the flexible units of alternating polyester−amides consisting of terephthalic acid, bis(esterdiamide)s, and aliphatic diols has been shown to influence the thermal and mechanical properties of these systems.[2−4]

The general structure of segmented block copolymers is $(A-B)_n$, where A and B are blocks of two dissimilar polymers chains. One of the segments is usually chosen to have the properties of a rubber (low T_g values). The hard segment forms the crystalline phase and acts as reinforcement to the elastomeric matrix. Some physicochemical properties of a series of polyester−amide−polyether segmented block copolymers have been reported.[5] The melting and glass transition temperatures of segmented copolymers with polyester−amide units of uniform length have been shown to vary with the soft-block length.[6] Furthermore, the structure, the crystallization behavior, and the mechanical properties of segmented polyester−amide copolymers based on poly(butylene terephthalate) and a diamide of uniform length have been investigated.[7]

So far, there has been little research on the synthesis and properties of random copolyester−amides containing flexible spacers. The literature available is mainly concerned with aliphatic polyester−amides.[8,9] The random copolymerization of ester and amide segments appears as an alternative route to yield materials with a combination of elastomeric and thermoplastic properties. Recently, novel random aromatic−aliphatic polyester−amide copolymers have been synthesized in our laboratory.[10] These materials possess a hetero-phase structure, with two T_g values and only one melting temperature above room temperature which corresponds to the fusion of poly(butylene terephthalate) (PBT) crystals. The diamide segments are chosen to mainly contribute to the amorphous domains and confer to the material an elastomeric character. The nanostructure of these materials and their correlation to physical properties has not yet been investigated.

Microindentation hardness has been shown to provide valuable information on the polymer nanostructure.[11,12] This method relies on the local deformation induced on a polymer surface with a sharp indenter under the application of a given load. The microhardness value can be determined from the optical measurement of the residual impression left behind upon load release. Microhardness is a simple, rapid, and nondestructive technique for the mechanical characterization of a material. From a basic point of view, much effort has been done in the past decades to correlate microhardness with the morphology and nanostructure of polymers, copolymers, polymer blends, and composites.[13−16] It has been shown that the microhardness of copolymer systems, including thermoplastic elastomers, thermotropic liquid-crystalline copolyesters, and random copolymers of semiflexible monomer units, is well described by a simple additive model of the microhardness of the individual components.[16] The microhardness of the latter is ultimately related to the corresponding

[†] Instituto de Estructura de la Materia (CSIC).
[‡] Technical University of Szczecin.
[§] Universität Hamburg.

10.1021/ma010199f CCC: $20.00 © 2001 American Chemical Society
Published on Web 10/12/2001

Scheme 1

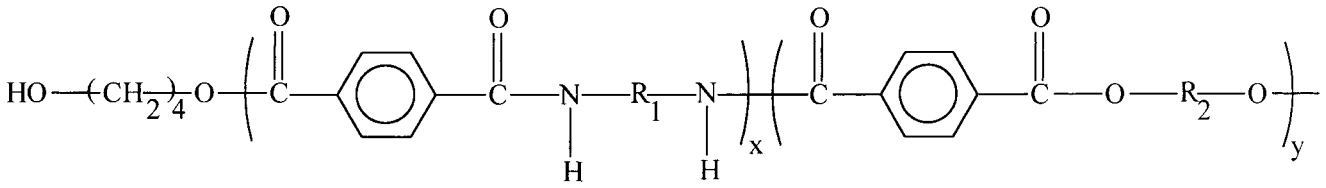

x, y - molar contents of the amide and the ester units respectively y / x = 3 - 49

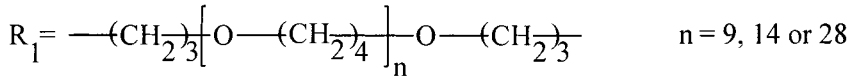

n = 9, 14 or 28

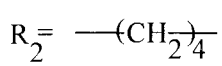

Table 1. Glass Transition Temperature, T_g, Melting Temperature, T_m, and Density, ρ, Values for the Polyester−Amide Samples with Different Molecular Weight of the α,ω-Di(3-aminopropyl)oligotetrahydrofuran Group, M_n, and Molar Content of Etherdiamide, ϕ^{DA} ($\phi^{DA} = x$ in Scheme 1)

M_n, g/mol	ϕ^{DA}, %	T_{g1}, °C	T_{m1}, °C	T_{g2}, °C	T_{m2}, °C	ρ, g/cm^3
	0			42	215, *225*	1.32
750	6	−38		35	205, *216*	1.27
750	14	−44		38	190, *199*, 210	1.21
750	20	−48		36	*183*, 200	1.17
750	25	−45		37	153	1.15
1100	4	−60		21	206, *218*	1.26
1100	11	−62		36	197, *205*, 212	1.20
1100	14	−61		39	173, *187*, 204	1.19
1100	20	−60		40	155, *166*, 186	1.15
2100	2	−60		43	212, *222*	1.23
2100	6	−69	20	45	208, *218*	1.18
2100	9	−70	18	47	205, *214*	1.13
2100	11	−72	12	38	171, *199*, 212	1.10

degree of crystallinity, crystalline lamellar thickness, and crystal surface free energy.[16−20]

The aim of the present paper is twofold: (1) to examine the correlation between the nanostructure, as derived from X-ray scattering, and the micromechanical properties of a series of newly synthesized random ester−amide copolymers, based on butylene terephthalate and an etherdiamide; (2) to study the influence of the number of flexible groups in the diamide units and the effect of the diamide content on the nanostructure and microhardness of the copolyester−amides.

Experimental Section

Polymer Synthesis. Novel polyester−amide copolymers were prepared by transesterification and polycondensation in the molten state. All polymers were synthesized with dimethyl terephthalate, 1,4-butanediol, and α,ω-di(3-aminopropyl)oligotetrahydrofuran. Scheme 1 illustrates the chemical formula of these newly synthesized polyester−amide copolymers. The final state of these copolymers is given by random-length sequences of etherdiamide and butyl terephthalate units. A number of 9, 14, and 28 tetrahydrofuran units were used in the oligotetrahydrofuran synthesis, yielding molecular weight values for the α,ω-di(3-aminopropyl)oligotetrahydrofuran group of M_n = 750 g/mol, M_n = 1100 g/mol, and M_n = 2100 g/mol, respectively. Samples with different etherdiamide molar content, ϕ^{DA}, were synthesized for each molecular weight of the α,ω-di(3-aminopropyl)oligotetrahydrofuran group (see Table 1). Magnesium hydrohexabutoxytitanate and phenol derivative Irganox 1098 were used as a catalyst and a stabilizing agent, respectively. A detailed description of the synthesis method can be found elsewhere.[10]

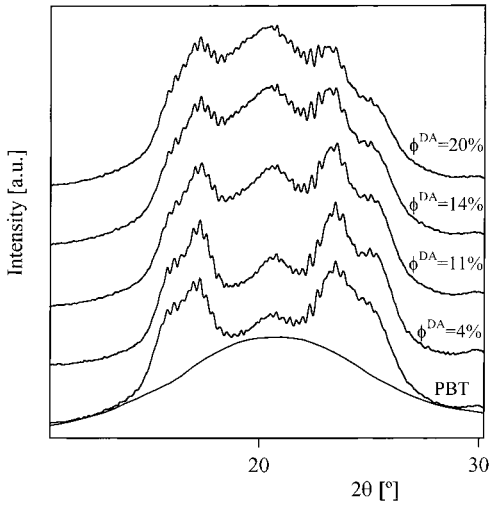

Figure 1. WAXS patterns of the PBT homopolymer and the copolyester−amide series with M_n = 1100 g/mol.

Sample Preparation. Pellets of the as-synthesized material were dried for 48 h at 70 °C under a pressure of ≈20 mbar. Injection molded samples with a circular shape were obtained using a Boy 15 injection-molding machine. The pressure applied was of 10 MPa, and the temperature of the melt used was 5 °C above the corresponding melting point of the polymer.

Techniques. Differential scanning calorimetry (DSC) data were obtained on a Perkin-Elmer DSC-7 in the range from −120 to +250 °C, using a heating and cooling rate of 10 °C/min. Table 1 collects the glass transition temperature, T_g, of the etherdiamide and the butylene terephthalate molecular segments and the melting temperature, T_m, of the PBT crystals for all the samples investigated. The italicized T_m values in Table 1 correspond to the melting temperature of the main PBT endothermic peak.

Density was measured at 22 °C, using an analytical balance equipped with a density determination apparatus (ISO 1183: 1987: "Plastics. Methods for determining of density and relative density of non-cellular plastics").

Wide-angle and small-angle X-ray diffraction patterns (WAXS, SAXS) were obtained using the synchrotron radiation source in the polymer beam-line of HASYLAB (DESY) in Hamburg. Scattering patterns were recorded using a one-dimensional detector. A wavelength, λ, of 0.15 nm was used. The data were corrected for the detector response and beam intensity. WAXS and SAXS patterns were calibrated against PET and rattail standards, respectively. Figure 1 shows the WAXS patterns of the PBT homopolymer and the copolyester−amide series with M_n = 1100 g/mol. Figure 2 illustrates the SAXS raw data for pure PBT and the copolymer series with M_n = 2100 g/mol. The small-angle X-ray scattered intensity,

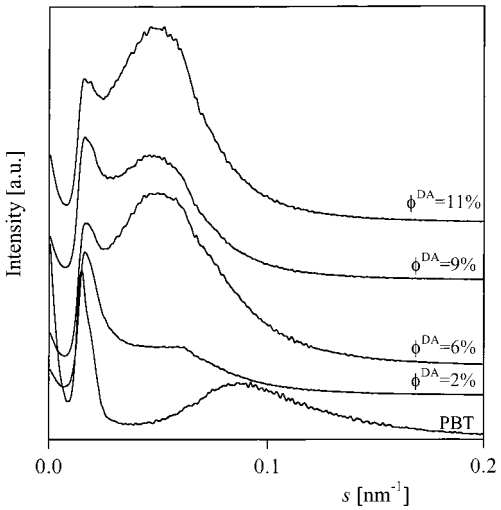

Figure 2. SAXS curves of the PBT homopolymer and the ester−amide copolymer series with M_n = 2100 g/mol. The intensity of all curves has been normalized to that of the homopolymer.

$I(s)$, was recorded in the interval 0.01 nm^{-1}< s < 0.2 nm^{-1}, with $s = 2 \sin \theta/\lambda$ being the modulus of the scattering vector.

The weight fraction crystallinity, w_c, was determined from the WAXS patterns. The amorphous peak, comprising the fraction of noncrystalline PBT material together with the contribution of the etherdiamide component, was fitted to the diffraction curve so that it matched at some points. The weight fraction crystallinity is calculated as the ratio between the area under the PBT crystalline peaks to that of the total diffraction curve. As an example, Figure 1 illustrates the amorphous halo fitted to the PBT homopolymer.

Microindentation measurements were performed at room temperature (23 °C) using a Leitz tester and a Vickers diamond indenter. Loads of 0.98 and 1.96 N were applied for 6 s and subsequently released to measure the residual area of indentation. Microhardness is determined from the slope of the linear regression of the load, P, vs d^2 plot (d is the diagonal of the indentation) according to the expression[16] $H = 1.854P/d^2$.

Evaluation of the SAXS Data. The average values of the long period and thicknesses of the amorphous and crystalline layers were determined from the interface distribution function (IDF), $g_1(x)$.[21] The IDF represents the probability distribution of finding two interfaces (between a crystal and the adjacent amorphous region) at a distance x from each other. The IDF is proportional to the second derivative of the one-dimensional correlation function, $\gamma_1(x)$.[22] To compute $g_1(x)$, the following steps were performed. Bearing in mind Porod's law, $s^4I(s)$ was computed and a slowly varying background was subtracted, yielding the interference function $G_1(s)$. One-dimensional Fourier transformation of $G_1(s)$ resulted in $g_1(x)$. The interface distribution function of each sample was fitted to Gaussian-type distributions, assuming the statistical model of flat and extended lamellar stacks.[23] The Gaussian functions provide for a simple mathematical treatment and fitted the experimental data very well. The IDF allows for the determination of the average thickness values of the crystalline, l_c, and amorphous layers, l_a, within the semicrystalline stacks. It has been shown that the relative width of the distribution of crystal thicknesses is, in general, the narrower one.[24,25] Thus, for each IDF, the Gaussian distribution with the smallest relative variance was associated with the crystalline layers (relative variance, $\sigma_c/l_c = 0.2-0.3$). The relative width of the Gaussian distribution associated with the amorphous layers varied in the range $\sigma_a/l_a = 0.5-0.6$.

Figure 3 shows the IDF for one of the samples (M_n = 1100 g/mol, ϕ^{DA} = 11%) together with the fitted model curve (solid line) and the Gaussian distributions of the amorphous and crystalline lamellae (dashed lines).

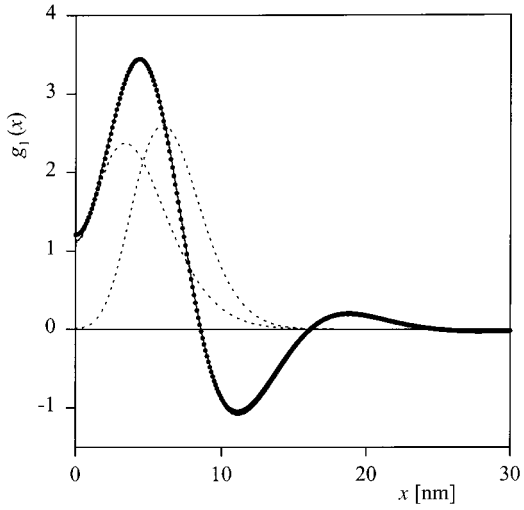

Figure 3. Interface distribution function (solid circles) and Gaussian-type distance distributions (dashed lines) for the copolyester-amide with ϕ^{DA} = 0.11 and M_n = 1100 g/mol. The solid line represents the curve fitted to the interface distribution function using a nonlinear regression.

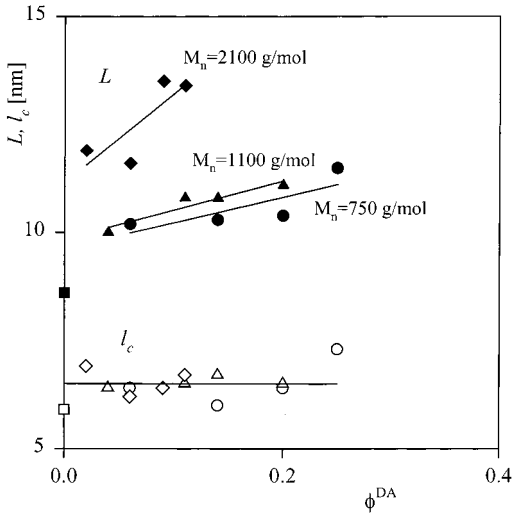

Figure 4. Variation of the long period (solid circles) and the crystal thickness (open circles) values with etherdiamide content for the PBT homopolymer (■, □) and the copolyester−amides with M_n = 750 g/mol (●, ○), M_n = 1100 g/mol (▲, △), and M_n = 2100 g/mol (◆, ◇).

Results

Wide-Angle and Small-Angle X-ray Scattering. Figure 4 illustrates the values of the long period, L, and the crystalline lamellar thickness, l_c, for all the copolymers investigated, as a function of ϕ^{DA}. The interface distribution function reveals that only two adjacent crystal lamellae contribute to the SAXS diffraction maxima. L is shown to increase with increasing etherdiamide content, for a given M_n value. The introduction of longer flexible groups in the etherdiamide units (higher molecular weight) yields larger L values. On the other hand, the l_c values are shown to remain constant for all the molecular weights and etherdiamide contents considered.

In Figure 5, the variation of the linear degree of crystallinity, α_L ($\alpha_L = l_c/L$), with etherdiamide content, is shown. There is a trend of the α_L values to diminish with increasing ϕ_{DA} and increasing molecular weight. This result is a direct consequence of the thickening of

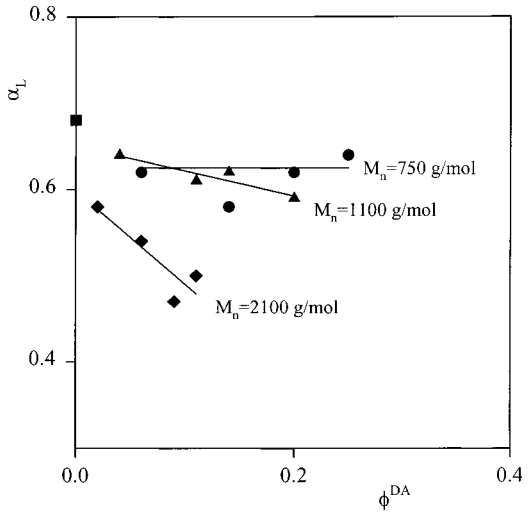

Figure 5. Plot of the linear degree of crystallinity as a function of etherdiamide content for pure PBT (■) and the copolyester−amides with M_n = 750 g/mol (●), M_n = 1100 g/mol (▲), and M_n = 2100 g/mol (◆).

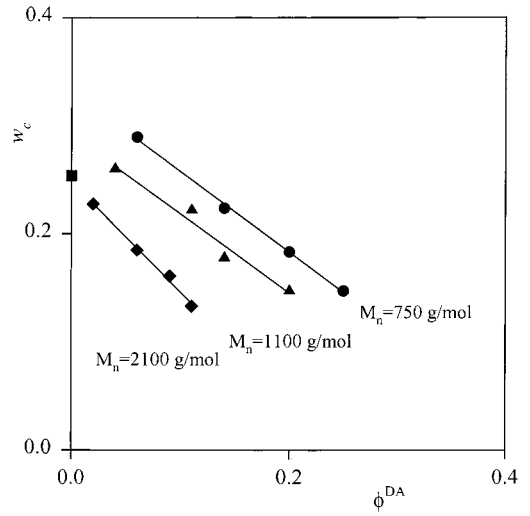

Figure 6. Weight fraction crystallinity vs etherdiamide content for all the copolyester−amide samples investigated and the PBT homopolymer. Symbols as in Figure 5.

the amorphous layer as the concentration or length of the etherdiamide units increases.

Figure 6 illustrates the mass degree of crystallinity values as a function of the molar etherdiamide content for the copolymers of different molecular weight and the PBT homopolymer. There is a clear trend of the w_c values to decrease with increasing etherdiamide content. In addition, Figure 6 shows that w_c values for the copolymers with M_n = 750 and 1100 g/mol and low etherdiamide contents ($\phi_{DA} \leq 6\%$) are slightly higher than that of the PBT homopolymer.

Microhardness Measurements. Figure 7 illustrates the hardness values for all the copolymers investigated (solid symbols) as a function of the etherdiamide content. The H value of the PBT homopolymer is also included in Figure 7. Hardness is shown to drastically decrease with increasing etherdiamide content. The hardness values of the copolymers clearly deviate from a linear additivity law (straight line in Figure 7), where we assume $H \approx 0$ for the polyetherdiamide homopolymer, as T_g is far below room temperature. The

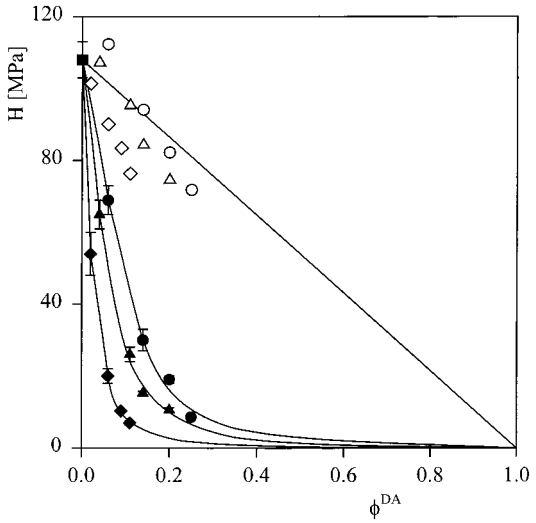

Figure 7. Plot of the experimental hardness values (solid circles) and calculated H data (open circles) as a function of etherdiamide content for the PBT homopolymer (■) and the copolyester−amides with M_n = 750 g/mol (●, ○), M_n = 1100 g/mol (▲, △), and M_n = 2100 g/mol (◆, ◇). The calculated hardness values are derived using eq 3, with H_c^{PBT} = 267 MPa, H_a^{PBT} = 54 MPa, and the corresponding v_c value of the individual samples. Solid curves are guide lines for the eye.

magnitude of this deviation is larger the higher the molecular weight of the copolymer is.

Discussion

Influence of Etherdiamide Content on the Nanostructure. The results shown in Figure 4 suggest that the crystallizable PBT sequences segregate to form the crystals while the etherdiamide sequences tend to lie in the amorphous phase. By increasing the amount or length of the etherdiamide sequences, the thickness of the intralamellar amorphous layer increases while the average PBT crystal thickness is preserved.

Figure 6 shows that the w_c values are much lower that the α_L values represented in Figure 5. This result suggests that a large proportion of amorphous material form regions outside the stacks of crystals. In addition, the w_c values for the copolymers with low etherdiamide contents ($\phi^{DA} \leq 6\%$) and M_n = 750 or 1100 g/mol are found to be larger that that of the PBT homopolymer. This finding could be associated with an enhanced mobility of the polymer chains due to the introduction of flexible sequences, which could facilitate the matching of neighboring crystallizable sequences. Finally, the trend of the w_c values to diminish with increasing ϕ^{DA} values parallels that of α_L (see Figure 5). However, in Figure 6 the crystallinity decrease appears to be more pronounced. Hence, the w_c decrease observed with increasing etherdiamide content could be partly due to a decrease in α_L. However, one cannot exclude the fact that a decreasing number of PBT crystallites with increasing ϕ^{DA} could also contribute to the w_c behavior observed.

Microhardness−Nanostructure Correlation. Figure 7 shows the conspicuous deviation of the H values of the copolymers from a linear additivity law. Similar results have been previously reported on other copolymer systems, where the hardness deviation from the linear additivity law was accounted for by taking into account that the hardness values of the individual components depart from those of the parent homo-

polymers.[16−20] To explain the H deviation observed in Figure 7 from the linear additivity law, let us introduce the following equation which describes the hardness of a two-component system in terms of the H values of the individual constituents:

$$H = H^{PBT}(1 - \phi^{DA}) + H^{DA}\phi^{DA} \quad (1)$$

Here, H^{PBT} and H^{DA} are the hardness values of the PBT and etherdiamide components, respectively ($H^{DA} \approx 0$). The value of H^{PBT} can be expressed in terms of the crystal hardness, $H_c{}^{PBT}$, the hardness of the PBT amorphous regions, $H_a{}^{PBT}$, and as a function of the volume degree of crystallinity of PBT referred to the volume fraction of the PBT component in the sample, $v_c{}^{PBT}$. Therefore, one can rewrite eq 1 to yield

$$H = [H_c{}^{PBT} v_c{}^{PBT} + H_a{}^{PBT}(1 - v_c{}^{PBT})](1 - \phi^{DA}) \quad (2)$$

Using the volume fraction crystallinity, $v_c = v_c{}^{PBT}(1 - \phi^{DA})$, eq 2 finally reads

$$H = H_c{}^{PBT} v_c + H_a{}^{PBT}(1 - v_c - \phi^{DA}) \quad (3)$$

$H_a{}^{PBT}$ has been reported to be of 54 MPa[19] and v_c values can be derived from the following relationship:

$$v_c = w_c \frac{\rho}{\rho_c} \quad (4)$$

where ρ_c is the crystal density of PBT (ρ_c = 1.404 g/cm^3)[26] and ρ and w_c data are taken from Table 1 and Figure 6, respectively.

On the other hand, the hardness of the crystals is known to depend on the crystal thickness through the following equation:[16]

$$H_c = \frac{H_c^{\infty}}{1 + \frac{b}{l_c}} \quad (5)$$

where $H_c{}^{\infty}$ is the crystal hardness of an infinitely thick crystal, which for PBT has been shown to be equal to 369 MPa,[19] and b is a parameter which is equal to the ratio between the surface free energy of the crystals, σ_e, and the energy required to plastically deform them, Δh:

$$b = \frac{2\sigma_e}{\Delta h} \quad (6)$$

Comparison of Experimental and Calculated Microhardness Data: Influence of Molecular Weight. Let us first assume that the b parameter is constant for all the samples investigated. Hence, H_c is constant throughout the series (l_c is constant as shown in Figure 4), and one can derive the $H_c{}^{PBT}$ value from the H and v_c data of the PBT homopolymer using eq 3 with $\phi^{DA} = 0$. This procedure yields a crystal hardness of $H_c{}^{PBT}$ = 267 MPa. Figure 7 includes the calculated microhardness data for the different copolyester−amides (open symbols) using eq 3 with $H_c{}^{PBT}$ = 267 MPa, $H_a{}^{PBT}$ = 54 MPa, and the corresponding v_c value for each copolymer. Figure 7 also shows that the calculated hardness values for all the etheramide/PBT copolymers are notably higher than the experimental ones. Hence, the variation of the volume degree of crystallinity in the series of copolyester−amides is not sufficient to explain the large depression observed for the hardness values of the copolymers with respect to the linear additivity decrease of PBT with ϕ^{DA} (straight line).

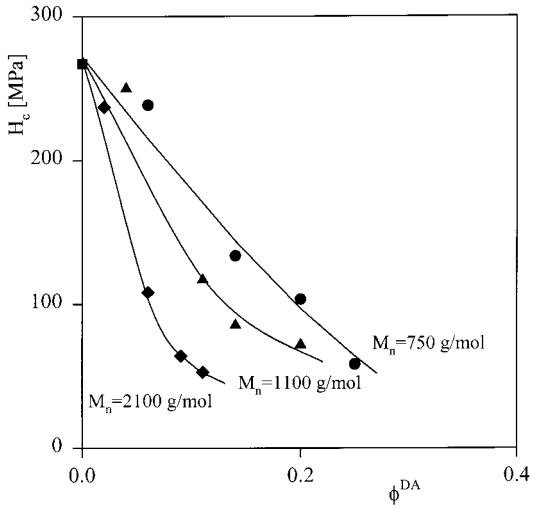

Figure 8. Variation of the crystal hardness values with etherdiamide content for pure PBT (■) and the copolyesteramides with M_n = 750 g/mol (●), M_n = 1100 g/mol (▲), and M_n = 2100 g/mol (◆). The H_c values for the copolyester−amides have been derived using eq 3 with $H_a{}^{PBT} = 0$.

There are three possibilities to account for the large deviation observed between the hardness calculated values and the experimental ones: (i) $H_a{}^{PBT}$ for the copolymers is different from that of the PBT homopolymer; (ii) $H_c{}^{PBT}$ varies with etherdiamide content, and this would be eventually related to a variation in the b parameter; (iii) both the $H_a{}^{PBT}$ and $H_c{}^{PBT}$ values for the copolymers are different from those for PBT. A quick look to the hardness data of the samples with the largest etherdiamide content (see Figure 7) reveals that these values are already smaller than the calculated contribution of the amorphous part to the hardness of the material (see eq 3, $H_a{}^{PBT}$ = 54 MPa). This result suggests that the $H_a{}^{PBT}$ value of the copolymers must be much lower than that of the homopolymer ($H_a{}^{PBT}$ = 54 MPa). The coexistence of etherdiamide and PBT segments within the amorphous regions seems to lower the hardness value of the PBT amorphous component. One could assume that the amorphous etherdiamide component resembles the characteristics of a liquid. In this case, the resistance of the amorphous PBT segments to plastic deformation should be reduced.

Let us then suppose that $H_a{}^{PBT} \approx 0$. Figure 8 shows the $H_c{}^{PBT}$ values for all the copolyester−amides, derived using eq 3 with $H_a{}^{PBT} \approx 0$. Crystal hardness is shown to decrease with increasing etherdiamide content for the three different molecular weights. This behavior must be ascribed to a change in the b parameter values with etherdiamide content (see eq 5).

Variation of the Crystal Surface Free Energy with Etherdiamide Content. Figure 9 shows the b values calculated for all the samples investigated. The b parameter is shown to increase with increasing etherdiamide content, the rate of increase being higher for the highest molecular weight. What could be the reason for this behavior? The b parameter is defined to measure of the ratio between the surface free energy of the crystals and the energy required to plastically deform them (see eq 6). Hence, the b param-

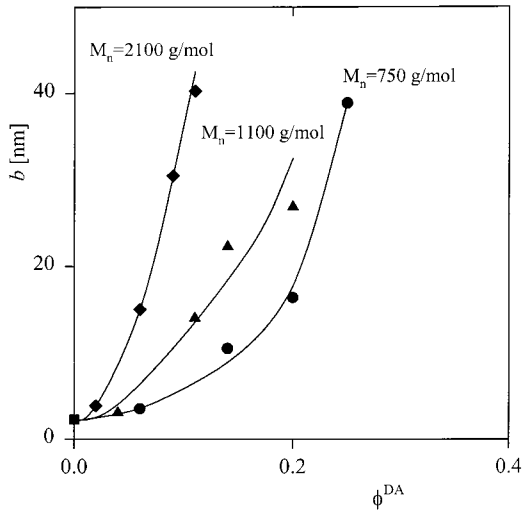

Figure 9. Plot of the *b* parameter values as a function of ϕ^{DA} for the PBT homopolymer and the ester−amide copolymers. Symbols as in Figure 8.

eter behavior observed in Figure 9 should be a consequence of a variation of σ_e and/or Δh with ϕ^{DA} and with the length of the flexible groups in the etherdiamide unit. To elucidate which one of the two factors, σ_e or Δh, is responsible for the observed *b* behavior, the values of the surface free energy of the lamellar crystals have been independently determined from calorimetric measurements using the Thomson−Gibbs equation:

$$T_m = T_m^0\left(1 - \frac{b^*}{l_c}\right) \tag{7}$$

Here, T_m^0 is the equilibrium melting equilibrium temperature and $b^* = 2\sigma_e/\Delta h_f^0$, where Δh_f^0 is the equilibrium melting enthalpy. We have pointed out before[27,28] that eqs 5 and 7 are analogous, the former describing the deviation of the crystal microhardness from the equilibrium mechanical properties through l_c and the mechanical *b* parameter, while the latter accounts for the T_m depression from the thermal equilibrium properties through l_c and the thermodynamical b^* parameter.

Figure 10a shows the σ_e values calculated for all the samples investigated, using eq 7, with the T_m values collected in Table 1 and $T_m^0 = 518$ K, $\Delta h_f^0 = 32$ kJ/mol.[29] The resulting plot shows that the crystal surface free energy is a monotonically increasing function of the etherdiamide content. This result suggests that as the content of noncrystallizable units increases, the concentration of defects at the crystal surface increases. On the other hand, the σ_e values are shown to be independent of the number of flexible units in the etherdiamide comonomer (see Figure 10a). Hence, the observed variation of the *b* parameter with molecular weight of the etherdiamide group must be explained in terms of a variation in the Δh parameter.

Figure 10b illustrates the plot of the b/b^* ratio vs ϕ^{DA} for the different molecular weights. The b/b^* value gives a measure of the ratio between the enthalpy required for the melting of the crystals and that necessary to plastically deform them ($b/b^* = \Delta h_f^0/\Delta h$). For the PBT homopolymer, $b/b^* \approx 10$ (see Figure 10b). Previous investigations have shown that the b/b^* ratio decreases with increasing chain stiffness.[28] In flexible polymers, the energy required for crystal deformation is much lower than the melting enthalpy. Values of $b/b^* = 30-45$ and $b/b^* = 2$ have been reported for PE and PET, respectively.[28] A b/b^* ratio of 10 for PBT, which possesses a chain stiffness in between that of PE and PET, is in agreement with these findings. In addition, Figure 10b shows that the $\Delta h_f^0/\Delta h$ ratio increases with increasing molecular weight and content of the etherdiamide component. As Δh_f^0 is a constant value for all the samples, the $\Delta h_f^0/\Delta h$ behavior observed must be due to a decrease in the Δh value as the molecular weight and content of the etherdiamide component increase. This effect could be explained on the basis of the occurrence of tie molecules connecting adjacent crystalline lamellae. It has been shown that the thickness of the amorphous regions in between crystals increases with increasing etherdiamide content and number of flexible groups in the etherdiamide units (see Figure 4). On the other hand, one would expect the etherdiamide segments within the amorphous layers to be largely entangled, especially when the etherdiamide unit contains lengthy flexible groups (high molecular weight). Therefore, tie molecules would have to surpass a highly entangled amorphous layer which thickens with increasing content and increasing molecular weight of the etherdiamide. Hence, it seems reasonable to assume that the number of tie molecules should tend to decrease with increasing ϕ^{DA} and increasing molecular weight of the etherdiamide. As tie molecules provide a mechanical reinforcement to the material, Δh values would decrease with increasing etherdiamide content and molecular weight of the etherdiamide comonomer.

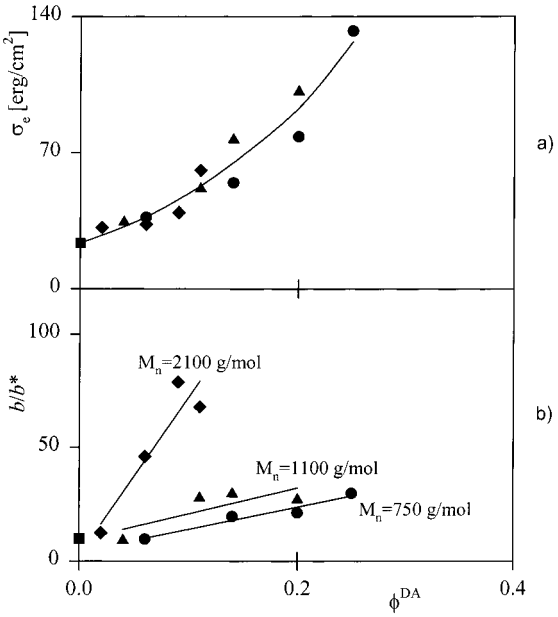

Figure 10. Plot of the crystal surface free energy (a) and the b/b^* ratio (b) vs etheramide content in the ester−amide copolymers. Symbols as in Figure 8.

Conclusions

1. The analysis of the interface distribution function from SAXS measurements on a series of etherdiamide/PBT copolymers reveals that the long period increases with increasing etherdiamide content and length of the flexible etherdiamide units while the crystal thickness is shown to remain constant. Results suggest that the crystallizable PBT sequences segregate to form the crystals while the etherdiamide sequences lie in the amorphous phase. Lamellae stacks comprise only two adjacent crystals.

2. The weight fraction crystallinity is shown to be much lower that the linear degree of crystallinity, indicating that a large proportion of amorphous material form regions outside the lamellae stacks. Both w_c and α_L values are shown to diminish with increasing etheramide content and increasing number of flexible groups in the etherdiamide unit.

3. Hardness values of the copolyester−amides are shown to largely deviate from the linear additivity law. This deviation can be accounted for by taking into account that the hardness values of the individual components depart from those of the parent homopolymers.

4. The dramatic decrease in the hardness values of the copolymers with respect to the PBT homopolymer is shown to be mainly due to (i) a lower hardness value of the PBT amorphous segments ($H_a^{PBT} \approx 0$) with respect to that of the PBT homopolymer ($H_a^{PBT} = 54$ MPa) and (ii) a crystal hardness values decrease with increasing etherdiamide content and increasing molecular weight of the etherdiamide unit. This result is a consequence of an increase in the mechanical *b* parameter with increasing ϕ^{DA}, the rate of increase being dependent on the molecular weight of the etherdiamide.

Acknowledgment. Grateful acknowledgment is due to MCYT (Grant BFM2000-1474) for the support of this investigation. A.F. also thanks the Comunidad Autónoma de Madrid for the award of a postdoctoral grant. The SAXS and WAXS measurements carried out at HASYLAB, DESY, Hamburg, have been funded by the TMR-Contract ERBFMGECT950059 of the European Community.

References and Notes

(1) Aharoni, S. M. *Macromolecules* **1988**, *21*, 1941.
(2) Gaymans, R. J.; de Haan, J. L.; van Nieuwenhuize, O. *J. Polym. Sci., Polym. Chem.* **1993**, *31*, 575.
(3) Serrano, P. J. M.; Thüss, E.; Gaymans, R. J. *Polymer* **1997**, *38*, 3893.
(4) Serrano, P. J. M.; van de Werff, B. A.; Gaymans, R. J. *Polymer* **1998**, *39*, 83.
(5) Sorta, E.; della Fortuna, G. *Polymer* **1980**, *21*, 728.
(6) Gaymans, R. J.; Haan, J. L. *Polymer* **1993**, *34*, 4360.
(7) van Bennekom, A. C. M.; Gaymans, R. J. *Polymer* **1997**, *38*, 657.
(8) Castaldo, L.; de Candia, F.; Maglio, G.; Palumbo, R.; Strazza, G. *J. Appl. Polym. Sci.* **1982**, *27*, 1809.
(9) Goodman, I.; Valavanidis, A. *Eur. Polym. J.* **1984**, *20*, 241.
(10) Pietkiewicz, D.; Roslaniec, Z. *Polimery* **1999**, *44*, 115.
(11) Baltá Calleja, F. J.; Santa Cruz, C.; Sawatari, C.; Asano, T. *Macromolecules* **1990**, *23*, 5352.
(12) Baltá Calleja, F. J. *Trends Polym. Sci.* **1994**, *2*, 419.
(13) Deslandes, Y.; Boudreau, F. *High Perform. Polym.* **1992**, *4*, 109.
(14) Osawa, S.; Porter, R. S. *Polymer* **1996**, *37*, 2095.
(15) Baltá Calleja, F. J.; Fakirov, S. *Trends Polym. Sci.* **1997**, *5*, 246.
(16) Baltá Calleja, F. J.; Fakirov, S. *Microhardness of Polymers*; Cambridge University Press: Cambridge, U.K., 2000.
(17) Baltá Calleja, F. J.; Santa Cruz, C.; Chen, D.; Zachmann, H. G. *Polymer* **1991**, *32*, 2252.
(18) Santa Cruz, C.; Baltá Calleja, F. J.; Zachmann, H. G.; Chen, D. *J. Mater. Sci.* **1992**, *27*, 2161.
(19) Giri, L.; Roslaniec, Z.; Ezquerra, T. A.; Baltá Calleja, F. J. *J. Macromol. Sci., Phys.* **1997**, *36*, 335.
(20) Baltá Calleja, F. J.; Fakirov, S.; Roslaniec, Z.; Krumova, M.; Ezquerra, T. A.; Rueda, D. R. *J. Macromol. Sci., Phys.* **1998**, *37*, 219.
(21) Ruland, W. *Colloid Polym. Sci.* **1977**, *255*, 417.
(22) Vonk, C. G.; Kortleve, G. *Kolloid Z. Z. Polym.* **1967**, *220*, 19.
(23) Stribeck, N. *Colloid Polym. Sci.* **1993**, *271*, 1007.
(24) Stribeck, N.; Alamo, R. G.; Mandelkern, L.; Zachmann, H. G. *Macromolecules* **1995**, *28*, 5029.
(25) Stribeck, N.; Zachmann, H. G.; Bayer, R. K.; Baltá Calleja, F. J. *J. Mater. Sci.* **1997**, *32*, 1639.
(26) Yokouchi, M.; Sakakibara, Y.; Chatani, Y.; Tadakoro, H.; Tanaka, T.; Yoda, K. *Macromolecules* **1976**, *9*, 266.
(27) Baltá Calleja, F. J.; Santa Cruz, C.; Kilian, H. G. *Colloid Polym. Sci.* **1990**, *268*, 440.
(28) Flores, A.; Baltá Calleja, F. J.; Bassett, D. C. *J. Polym. Sci., Polym. Phys.* **1999**, *37*, 3151.
(29) Cheng, S. Z. D.; Pan, R.; Wunderlich, B. *Makromol. Chem.* **1988**, *189*, 2443.

MA010199F